Quantitative analysis of InAs quantum dot solar cells by photoluminescence spectroscopy

Ryo Tamaki, Yasushi Shoji, Laurent Lombez, Jean-François Guillemoles, Yoshitaka Okada

▶ **To cite this version:**

Ryo Tamaki, Yasushi Shoji, Laurent Lombez, Jean-François Guillemoles, Yoshitaka Okada. Quantitative analysis of InAs quantum dot solar cells by photoluminescence spectroscopy. Photonics WEST - SPIE 2018, Jan 2018, San Francisco, United States. 10.1117/12.2291465 . hal-03024118

HAL Id: hal-03024118
https://cnrs.hal.science/hal-03024118

Submitted on 3 Oct 2022

HAL is a multi-disciplinary open access archive for the deposit and dissemination of scientific research documents, whether they are published or not. The documents may come from teaching and research institutions in France or abroad, or from public or private research centers.

L'archive ouverte pluridisciplinaire **HAL**, est destinée au dépôt et à la diffusion de documents scientifiques de niveau recherche, publiés ou non, émanant des établissements d'enseignement et de recherche français ou étrangers, des laboratoires publics ou privés.

Quantitative analysis of InAs quantum dot solar cells by photoluminescence spectroscopy

Ryo Tamaki*[a,c], Yasushi Shoji[a,c], Laurent Lombez[b,c], Jean-François Guillemoles[b,c], and Yoshitaka Okada[a,c]

[a]Research Center for Advanced Science and Technology (RCAST), The University of Tokyo, 4-6-1 Komaba, Meguro-ku, Tokyo, Japan 153-8904; [b]Institut Photovoltaïque Ile de France (IPVF), UMR CNRS 9006, 30 route 128, Palaiseau, France 91120; [c]NextPV, LIA RCAST-CNRS, The University of Tokyo, 4-6-1 Komaba, Meguro-ku, Tokyo, Japan 153-8904

ABSTRACT

We have quantitatively investigated the two-step photon absorption in quantum dot solar cells (QDSCs) by using absolute intensity calibrated photoluminescence (PL) spectroscopy. Multi-stacked InAs/AlGaAs QDs were fabricated in the *i*-region of *p*-*i*-*n* single-junction solar cells by molecular beam epitaxy. Hyperspectral imaging, which combines both the spatial and spectral dimensions of the luminescence, was used to investigate QD ground state PL at room temperature. Two lasers simultaneously excited the QDSCs to characterize two-step photon absorption. An excitation laser caused interband transition to generate photo-carriers in QDs, and the other infrared (IR) laser excited intraband transition from the QD states. As the result of two-step photon absorption, reduction in PL intensity was clearly observed under IR bias excitation. We compared absolute PL intensity with and without IR illumination, and obtain quasi-Fermi level splitting and two-step photon absorption efficiency in QDSCs under study. Compared with the photocurrent measurements, PL spectroscopy performed under open-circuit conditions, so that higher carrier filling ratio can be realized in QDs. Furthermore, PL can characterize fundamental transition on two-step photon absorption because photocurrent production needs carrier extraction to the external circuit. Quantitative analysis of two-step photon absorption by PL spectroscopy could clarify physical insights, and it would be beneficial to realize high efficiency intermediate band solar cells.

Keywords: intermediate band solar cell, quantum dot solar cell, InAs quantum dot, photoluminescence spectroscopy, intersubband transition, III-V semiconductor

1. INTRODUCTION

Due to significant progress on research and development in photovoltaics, the world record efficiency in crystalline or thin-film solar cells[1,2] have been approaching to the theoretical efficiency limit.[3] III-V semiconductor multi-junction solar cells are the best performing device architecture, which the highest certified efficiency of laboratory cells is 46.0% under 508 suns.[1,2] However, because they are composed of epitaxially grown and/or wafer bonded stacked sub-cells, there are many constraints for practical applications and further efficiency gain. As next generation solar cells, new physical concepts have been proposed to overcome the limiting efficiency of single-junction solar cells. We have explored III-V quantum dot solar cells (QDSCs) as a promising candidate for intermediate band solar cells (IBSCs). In IBSCs, an additional sub-bandgap level, that is the IB, in the host single-junction solar cell can reduce transmission losses.[4,5] In addition to the interband transitions from the valence band (VB) to the conduction band (CB), two-step photon absorption via the IB can convert below-bandgap infrared (IR) photons to photocurrent.[6,7]

In last decade, many efforts have been made to realize efficient two-step photon absorption in IBSCs.[8] However, to achieve high efficiency in IBSCs, both two-step photon absorption and voltage preservation should be realized simultaneously. In usual, insertion of the IB results in increase of recombination pathways, therefore, output voltage of the solar cell is significantly degraded. In the currently available IBSCs, the gain in photocurrent is inferior to the voltage degradation.[9] It is obvious that degradation in the open-circuit voltage with the introduction of QDs. However, it is not straightforward to understand the physics behind. In this study, we have performed absolute intensity calibrated photoluminescence (PL) spectroscopy to evaluate the quasi-Fermi level splitting directly in QD-IBSCs.

*E-mail: tamaki@mbe.rcast.u-tokyo.ac.jp

In addition, there is an issue to realize two-step photon absorption at ambient conditions. Thermionic emission of photo-carriers out of QDs is the dominant process that reduces population of QDs to absorb IR photons. In general, external quantum efficiency difference with and without IR irradiation, that is the ΔEQE, is characterized to quantify the photocurrent gain via two-step photon absorption. In conventional In(Ga)As/GaAs QD systems, enhancement in EQE under IR bias illumination was confirmed in previous studies.[10,11,12] However, the band alignment of the InAs/GaAs QDs is not optimized for IBSC because wide bandgap host is preferable both for spectral matching for sun-light spectrum and reduction of thermionic emission of photo-carriers out of QD states.

In ΔEQE measurement, carrier extraction to the external circuit is necessary to measure as photocurrent, therefore, fundamental transition of IR photon absorption cannot investigate directly. In previous works, fundamental transition of IR photon absorption was observed by the quenching of PL intensity by time-resolved spectroscopy.[13,14] In InAs/GaAs QD system, absorption coefficient of IR photon absorption was estimated to be 600 cm^{-1} for the fundamental state of QDs with full filled conditions.[14] In our previous study, we observed PL reduction by IR photo-irradiation under continuous wave (CW) excitation.[15] It is obvious that PL quenching of the QD luminescence with IR irradiation, but comparison between different QD structure and quantitative analysis have not been studied in detail. In this study, we have performed absolute intensity calibrated PL spectroscopy to investigate the fundamental transition of two-step photon absorption in InAs QD systems with wide bandgap host matrix layers.

2. EXPERIMENT

2.1 InAs QDSCs with wide bandgap AlGaAs host matrix

Multi-stacked (20 stacks) InAs QD layers were embedded in the *i*-region of the host *p*-*i*-*n* single-junction solar cells on *n*-GaAs substrates by solid-source molecular beam epitaxy (MBE). To increase the band offset between the QD confinement states and the CB edge of the host materials, $Al_xGa_{1-x}As$ (x=0.2, 0.4)[16,17] were utilized as the host matrix layers. The bandgap energies at room temperature (RT) of the host materials were 1.70 eV and 1.97 eV for $Al_{0.2}Ga_{0.8}As$, and $Al_{0.4}Ga_{0.6}As$, respectively. Typical InAs QD ground state emission appeared at around 1.0 μm (1.24 eV) at RT for QDSCs under study. The detail device structures of the QDSCs are schematically shown in Fig 1. In the following PL experiments, the devices were remained at open-circuit conditions.

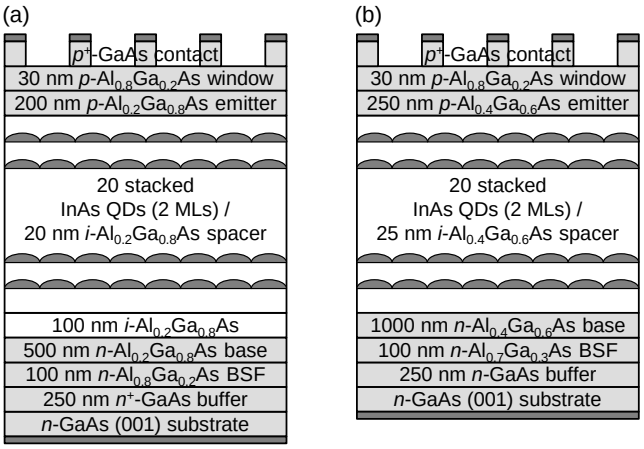

Figure 1. Schematic illustrations of (a) InAs/$Al_{0.2}Ga_{0.8}As$ and (b) InAs/$Al_{0.4}Ga_{0.6}As$ QDSC structures.

2.2 Hyperspectral imaging with absolute PL intensity calibration

Absolute intensity calibrated PL spectroscopy was conducted by using a hyperspectral imager (Photon etc.). Hyperspectral imaging combines both the spatial and spectral dimensions of the luminescence.[18] A schematic illustration of the optical setup is shown in Fig. 2. An InGaAs camera was attached on the hyperspectral imager to detect luminescence longer than 950 nm (1.31 eV). Two CW lasers simultaneously excited the sample. A laser with the wavelength at 786.3 nm (1.58 eV) could not directly excite AlGaAs layers because the photon energy was below the bandgap energy of host materials. The photon energy is between the QD ground state and the bandgap of AlGaAs,

therefore, interband transition for higher order quantized states or wetting layers was excited and generated photo-carriers in QDs. It is noted that the absorption coefficient at this excitation wavelength is small enough to homogeneously excite active region in the depth direction. In contrast, the other IR laser at 1550 nm (0.80 eV) could not excite any interband transition because the photon energy is sufficiently small, and intraband transition via two-step photon absorption occurred under additional IR bias light illumination.

To calibrate the relative PL intensity (arb. units) to the calibrated photon flux (photons/s/nm/cm^2), spectral, spatial, and absolute sensitivity were calibrated as follows.[19] First, relative calibration in the spatial and spectral dimensions was conducted. We used a calibrated halogen lamp coupled into an integrating sphere, which provide a spatially homogeneous output with known relative spectral intensity. A hyperspectral image of the output port of the integrating sphere provided calibration standard for the spatial and spectral relative sensitivity of the PL detection. Second, an absolute calibration was determined at a given wavelength. It was carried out by a laser at 1062.2 nm (1.17 eV) coupled in an optical fiber and imaging its output by the hyperspectral imager. It is noted that the laser wavelength was close to the range of QD PL spectra (950 - 1050 nm). The number of detecting counts on the InGaAs camera was compared with the actual intensity measured with a Ge photo-diode power meter. The angle dependence of the luminescence is assumed to be Lambertian, that is independent of the angle of emission, and the cosine factor for the solid angle of the microscope objective lens within its numerical aperture is deduced the correction angle of the optical system.

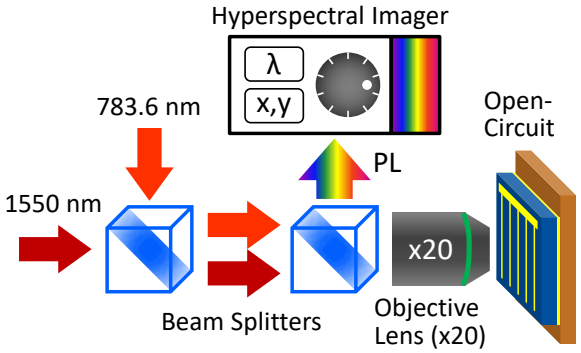

Figure 2. A schematic illustration of the optical setup of hyperspectral imaging with two excitation lasers.

3. RESTULS AND DISCUSSION

3.1 Absolute PL spectra on InAs/AlGaAs QDSCs

Absolute PL spectra of the InAs/AlGaAs QDSCs have been investigated as plotted in Fig. 3. The measurement temperature was at RT and the solar cells were kept at open-circuit conditions. In hyperspectral imaging, three-dimensional data with spatial (x,y) and spectral (λ) resolution can be obtained. The PL spectra were spatially averaged over whole excitation spot on the focal plane. Laser excitation intensities were 15 mW at 783.6 nm and 28 mW at 1550 nm, respectively. The spot diameter defined at $1/e^2$ intensity was about 65 μm. As the result, excitation densities were 460 W/cm^2 and 850 W/cm^2, respectively, at 783.6 nm and 1550 nm. Irradiated photon flux of the excitation lasers was equivalent to the order of 10,000 suns of Air Mass 1.5 spectrum.

As clearly shown in Fig. 3, PL peaks centered at around 1016 nm (1.22 eV) and 986 nm (1.26 eV) were observed, respectively, on InAs/$Al_{0.2}Ga_{0.8}$As and InAs/$Al_{0.4}Ga_{0.6}$As QDSCs. The PL peaks were assigned as luminescence from the QD ground states. The QD excited states or wetting layers were excited by the 786.3 nm (1.58 eV) excitation laser, and AlGaAs host matrix could not absorb excitation photons. The obtained PL signal is trapped carriers via fast relaxation of photo-carriers to the confined QD ground states, and it is not preferable as an IBSC because it causes energy (voltage) loss. On the other hand, additional IR bias light illumination at 1550 nm (0.80 eV) clearly reduced the PL intensity, $\Delta PL = PL_{w/o\ IR} - PL_{w/\ IR}$, from the QD ground states. The reduction ratio of the PL intensity, $\Delta PL/PL$, is about 3% and 5% in InAs/$Al_{0.2}Ga_{0.8}$As and InAs/$Al_{0.4}Ga_{0.6}$As QDSCs, respectively. It is attributed to two-step photon absorption of the QD electrons to the CB, which is desirable feature as an IBSC.

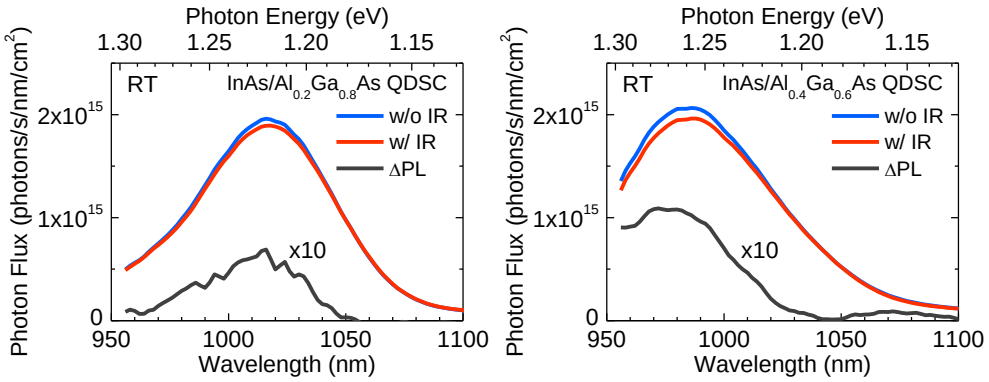

Figure 3. Absolute PL spectra on the InAs/AlGaAs QDSCs with and without IR bias (1550 nm) illumination at RT.

To analyze the absolute PL intensity and estimate quasi-Fermi level splitting, we utilized generalized Planck's law,[20]

$$\phi_{em}(\hbar\omega) = \alpha(\hbar\omega)\frac{\Omega}{4\pi^3\hbar^3c^2}\frac{(\hbar\omega)^2}{\exp\left(\frac{\hbar\omega-\Delta\mu}{k_BT}\right)-1}, \quad (1)$$

where ϕ_{em} is emission rate in a unit volume, resulting in a luminescence in a solid angle. $\hbar\omega$ is the photon energy, α is the absorbance, Ω is the solid angle, and $\Delta\mu$ is the quasi-Fermi level splitting. In the experimental setup in Fig. 1, we could observe a given surface area with a fixed solid angle, so that integration over the emitting volume is indispensable. In nanostructured solar cells, $\Delta\mu$ would not be constant in the depletion region because finite mobility of carriers through nanostructures. In this study, we simplified the device model to be a constant $\Delta\mu$ in all active region and evaluating effective $\Delta\mu_{eff}$ from the absolute PL measurements. Furthermore, Boltzmann approximation is applied to calculate (1) because $\hbar\omega - \Delta\mu \gg k_BT = 25.4$ meV is satisfied.

3.2 Absolute PL and Δμ maps on InAs/AlGaAs QDSCs

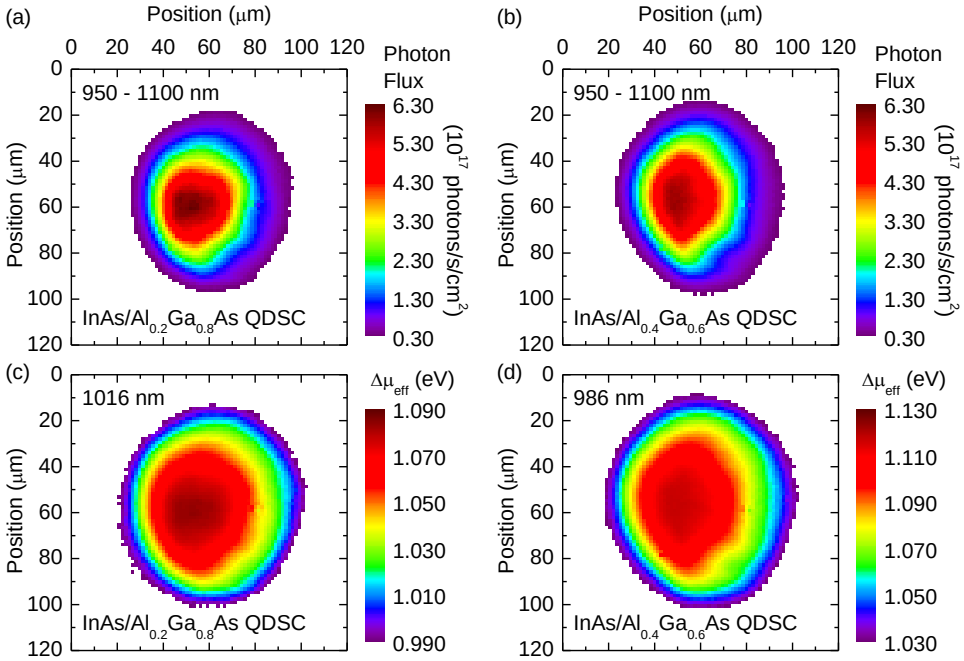

Figure 4. (a), (b) Absolute PL maps (spectral integrated) and (c), (d) $\Delta\mu_{eff}$ maps at QD PL peak wavelengths (at 1016 nm and 986 nm) on (a), (c) InAs/$Al_{0.2}Ga_{0.8}$As QDSC and (b), (d) InAs/$Al_{0.4}Ga_{0.6}$As QDSC at RT under 786.3 nm excitation.

The obtained absolute PL and $\Delta\mu_{eff}$ maps on the InAs/AlGaAs QDSCs are summarized in Fig. 4. The absolute PL map was obtained by integrating the luminescence for the spectral range from 950 to 1100 nm. On the other hand, the PL emission wavelengths at 1016 nm (1.22 eV) and 986 nm (1.26 eV), respectively, were utilized to calculate the $\Delta\mu_{eff}$ maps on InAs/$Al_{0.2}Ga_{0.8}$As and InAs/$Al_{0.4}Ga_{0.6}$As QDSCs. In the calculation using (1), we assumed that the temperature (T) remained at RT (293 K) and absorbance, α, was 0.01. The relevance of this assumption should be guaranteed in future study, but the error in the estimated $\Delta\mu_{eff}$ is 17.5 meV with a factor of two error in α. By comparing the spatially averaged $\Delta\mu_{eff}$ within the $1/e^2$ spot diameter, 1.050 eV and 1.084 eV was obtained in InAs/$Al_{0.2}Ga_{0.8}$As and InAs/$Al_{0.4}Ga_{0.6}$As QDSCs, respectively. The difference in these $\Delta\mu_{eff}$ of 34 meV is almost the same as the energy difference in QD PL peaks (37 meV) indicating the same population in QDs was generated in both QDSCs. On the other hand, the difference in $\Delta\mu_{eff}$ with and without IR bias light was estimated to be 0.9 meV in the InAs/$Al_{0.2}Ga_{0.8}$As QDSC and 1.3 meV in the InAs/$Al_{0.4}Ga_{0.6}$As QDSC. A subtle but clear change in $\Delta\mu_{eff}$ was confirmed under IR bias photo-irradiation via two-step photon absorption.

3.3 Quantitative analysis of two-step photon absorption and quasi-Fermi level splitting

Spatial and spectral integrated photon flux of QD luminescence can be investigated by analyzing Figs. 3 and 4. In both InAs/AlGaAs QDSCs, the total photon flux obtained by absolute PL measurements on the QDSCs was estimated to be about 3×10^{17} photons/s/cm^2. When the optically active areal QD density was 3×10^{10} cm^{-2} and the effective carrier lifetime was 1 ns, the occupation density of QDs by photo-carriers could be calculated to be 1%. The low occupancy of the QD ground states was consistent with no apparent excited state emission in the PL spectra shown in Fig. 3. As discussed in section 3.1, a few percent of ΔPL/PL were observed under IR bias light illumination, which corresponding to the reduction of QD emission about 1×10^{16} photons/s/cm^2. The irradiated IR bias light (1550 nm) density was 6.6×10^{21} photons/s/cm^2, therefore, absorption coefficient of bound-to-continuum transitions on two-step photon absorption was estimated to be the order of $\alpha_{QD\text{-}CB}$=100 cm^{-1} with full filled conditions. It is similar to experimentally[13,14] and theoretically[21,22] reported values. However, it is not sufficiently large to absorb all IR photons. It is necessary to increase the absorption cross section by increasing areal QD density and/or utilizing light-management technique.[23]

A possible interpretation for the $\Delta\mu_{eff}$ difference obtained under IR bias light illumination is schematically shown in Fig. 5. It is clear that the reduction of PL intensity under IR illumination indicating reduction of photo-carrier population in QDs, resulting reduction in $\Delta\mu_{eff}$ of about 1 meV. In addition, the population in CB might be increased due to two-step photon absorption, therefore, $\Delta\mu_{VC} = \mu_{CB} - \mu_{VB}$ between the VB and CB would be enhanced. As the result, $\Delta\mu_{QC} = \mu_{CB} - \mu_{QD}$ between the QD and CB might emerge under non-equilibrium conditions via two-step photon absorption.

The larger band offset is preferable for efficient two-step photon absorption against thermionic emissions of photo-carriers out of QDs. According to the ΔPL and $\Delta\mu_{eff}$ analysis, no significant difference was observed between InAs/$Al_{0.2}Ga_{0.8}$As and InAs/$Al_{0.4}Ga_{0.6}$As QDSCs, therefore as discussed before, the results indicated that the same population was generated in InAs QDs for both samples. Finally, the same order of absorption coefficient for bound-to-continuum transitions in two-step photon absorption was confirmed in InAs/AlGaAs QDSCs.

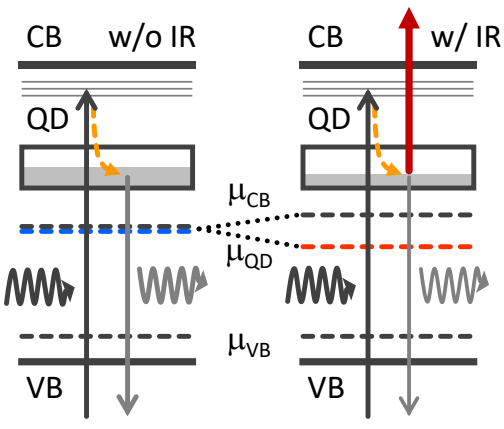

Figure 5. Schematic band diagrams of quasi-Fermi level splitting in QD system with and without IR bias light illumination.

4. SUMMARY

In this study, we performed absolute intensity calibrated PL spectroscopy to evaluate two-step photon absorption and quasi-Fermi level splitting in InAs/AlGaAs QDSCs to examine fundamental transition of two-step photon absorption and voltage preservation issue on QD-IBSCs. Reduction of the PL intensity from the QD ground state was clearly observed under additional IR bias light illumination. Generalized Planck's law was applied to calculate the $\Delta\mu_{eff}$ of the QDSC from absolute PL intensity. The change in $\Delta\mu_{eff}$ with and without IR bias light was estimated to be about 1 meV. A subtle but clear difference in $\Delta\mu_{eff}$ might be possible to interpret as the existence of quasi-Fermi level splitting between the QD and CB via two-step photon absorption. The absolute PL intensity made it possible to determine the QD carrier population and the absorption coefficient of two-step photon absorption. The obtained absorption coefficient at full filled condition was order of 100 cm^{-1} for bound-to-continuum transitions irrespective to the host AlGaAs bandgap energy.

There are remaining issues to interpret the data more accurately, such that non-uniform $\Delta\mu_{eff}$ in the spatial dimensions, quantitative absorbance at the resonance of the QD states, and direct observation of change in $\Delta\mu_{QC} = \mu_{CB} - \mu_{QD}$. Nonetheless, the obtained results quantified the amount of voltage gain via two-step photon absorption at RT. The $\Delta\mu_{eff}$ difference would possibly enhance more by optimizing the energy band alignment of the QD layers by band engineering using quantum heterostructures. Moreover, laser excitation density equivalent to 10,000 suns already exceeded the practical concentration conditions for concentrator photovoltaics (CPV), typically below 1,000 suns. Laser excitation density dependence varying the QD populations, or change in the ratio between interband and intraband transitions would be interesting to apply for absolute PL intensity characterization in nanostructured IBSCs to clarify the voltage recovery effect and solve the voltage preservation issue.

ACKNOWLEDGEMENTS

This work is performed under R&D on ultra-high-efficiency and low-cost III-V compound semiconductor photovoltaic cells and modules supported by National Research and Development Agency, New Energy and Industrial Technology Development Organization (NEDO). This work was partly supported by Ministry of Economy, Trade and Industry (METI), Japan and the Precise Measurement Technology Promotion Foundation (PMTP-F).

REFERENCES

[1] National Renewable Energy Laboratory (NREL), National Center for Photovoltaics, "Research cell efficiency records chart," http://www.nrel.gov/ncpv (30 October 2017).
[2] Green, M. A., Hishikawa, Y., Dunlop, E. D., Levi, D. H., Hohl-Ebinger, J. and Ho-Baillie, A. W. Y., "Solar cell efficiency tables (version 51)," Prog. Photovolt: Res. Appl. 24, 3-12 (2017).
[3] Shockley, W. and Queisser, H. J., "Detailed balance limit of efficiency of *p-n* junction solar cells," J. Appl. Phys. 32, 510-519 (1961).
[4] Wolf, M., "Limitations and Possibilities for Improvement of Photovoltaic Solar Energy Converters: Part I: Considerations for Earth's Surface Operation," Proc. IRE 48, 1246 (1960).
[5] Luque, A. and Martí, A., "Increasing the efficiency of ideal solar cells by photon induced transitions at intermediate levels," Phys. Rev. Lett. 78, 5014-5017 (1997).
[6] Martí, A., Antolín, E., Stanley, C. R., Farmer, C. D., López, N., Díaz, P., Cánovas, E., Linares, P. G. and Luque, A., "Production of photocurrent due to intermediate-to-conduction-band transitions: A demonstration of a key operating principle of the intermediate-band solar cell," Phys. Rev. Lett. 97, 247701 (2006).
[7] Okada, Y., Morioka, T., Yoshida, K., Oshima, R., Shoji, Y., Inoue, T. and Kita, T., "Increase in photocurrent by optical transitions via intermediate quantum states in direct-doped InAs/GaNAs strain-compensated quantum dot solar cell," J. Appl. Phys. 109, 024301 (2011).
[8] Okada, Y., Ekins-Daukes, N. J., Kita, T., Tamaki, R., Yoshida, M., Pusch, A., Hess, O., Phillips, C. C., Farrell, D. J., Yoshida, K., Ahsan, N., Shoji, Y., Sogabe, T. and Guillemoles, J.-F., "Intermediate band solar cells: Recent progress and future directions," Appl. Phys. Rev. 2, 021302 (2015).

[9] Luque, A., Martí, A. and Stanley, C., "Understanding intermediate-band solar cells," Nature Photon. 6, 146-152 (2012).
[10] Shoji, Y., Akimoto, K. and Okada, Y., "Self-organized InGaAs/GaAs quantum dot arrays for use in high-efficiency intermediate-band solar cells," J. Phys. D: Appl. Phys. 46, 024002 (2013).
[11] Shoji, Y., Narahara, K., Tanaka, H., Kita, T., Akimoto, K. and Okada, Y., "Effect of spacer layer thickness on multi-stacked InGaAs quantum dots grown on GaAs (311)B substrate for application to intermediate band solar cells," J. Appl. Phys. 111, 074305 (2012).
[12] Sogabe, T., Shoji, Y., Ohba, M., Yoshida, K., Tamaki, R., Hong, H.-F., Wu, C.-H., Kuo, C.-T., Tomić, S. and Okada, Y., "Intermediate-band dynamics of quantum dots solar cell in concentrator photovoltaic modules," Sci. Rep. 4, 4792 (2014).
[13] Kita, T., Maeda, T. and Harada, Y., "Carrier dynamics of the intermediate state in InAs/GaAs quantum dots coupled in a photonic cavity under two-photon excitation," Phys. Rev. B 86, 035301 (2012).
[14] Harada, Y., Maeda, T. and Kita, T., "Intraband carrier dynamics in InAs/GaAs quantum dots stimulated by bound-to continuum excitation," J. Appl. Phys. 113, 223511 (2013).
[15] Rale, P., Delamarre, A., El-Hajje, G., Tamaki, R., Watanabe, K., Shoji, Y., Okada, Y., Sugiyama, M., Lombez, L. and Guillemoles, J.-F., "Quantitative optical measurement of chemical potentials in intermediate band solar cells," J. Photon. Energy 5, 053092 (2015).
[16] Shoji, Y. and Okada, Y., "Effect of external bias on multi-stacked InAs/AlGaAs quantum dots solar cell," Proceedings of the 40th IEEE Photovoltaic Specialists Conference (PVSC), 1099-1102 (2014).
[17] Shoji, Y. and Okada, Y., "InGaAs quantum dot solar cells with high energygap matrix layers," Proceedings of the 39th IEEE Photovoltaic Specialists Conference (PVSC), 0314-0317 (2013).
[18] Delamarre, A., Lombez, L. and Guillemoles, J.-F., "Contactless mapping of saturation currents of solar cells by photo-luminescence," Appl. Phys. Lett. 100, 131108 (2012).
[19] Delamarre, A., Paire, M., Guillemoles, J.-F. and Lombez, L., "Quantitative luminescence mapping of Cu(In,Ga)Se_2 thin-film solar cells," Prog. in Photovolt.: Res. and Appl. 23, 1305-1312 (2015).
[20] Würfel, P., "The chemical potential of radiation," J. Phys. C: Solid Stat. Phys. 15, 3967-3985 (1982).
[21] Luque, A., Martí, A., Mellor, A., Marrón, D. F., Tobías, I. and Antolín, E., "Absorption coefficient for the intraband transitions in quantum dot materials," Prog. Photovolt: Res. Appl. 21, 658-667 (2013).
[22] Tomić, S., Sogabe, T. and Okada, Y., "In-plane coupling effect on absorption coefficients of InAs/GaAs quantum dots arrays for intermediate band solar cell," Prog. Photovolt: Res. Appl. 23, 546-558 (2015).
[23] Mellor, A., Luque, A., Tobías, I. and Martí, A., "The feasibility of high-efficiency InAs/GaAs quantum dot intermediate band solar cells," Sol. Energy Mater. Sol. Cells130, 255-233 (2014).